Space Sciences Laboratory
University of California
Berkeley, California 94720

Semi-Annual Report on

A STUDY OF ADVANCED INFRARED DETECTORS FOR USE IN PLANETARY SPECTROSCOPY

Supported by

NASA Grant

NsG 707

For the period

October 1, 1966 through March 31, 1967

Principal Investigator: Professor Harold Weaver

Space Sciences Laboratory Series No. 8, Issue No. 46
March 31, 1967

A STUDY OF ADVANCED INFRARED DETECTORS FOR USE IN PLANETARY SPECTROSCOPY

NASA Grant
NsG 707

I. SUMMARY OF WORK DURING THIS PERIOD

A. BOLOMETER FABRICATION

1. During the previous reporting period thirty-six bolometers were fabricated from one (Crystal No. 1) of the four germanium samples on hand.[1] About half of these units were lost in handling and in the process of working out mounting techniques (principally due to pulling a lead wire loose at the soldered connection to the germanium die). Some of the ruined bolometers have been replaced; currently, twenty-three units are available for use. In addition, two bolometers have been fabricated from the Crystal No. 1 material, using 0.002-inch brass wire for comparison with the potentiometer wire leads used earlier. As yet, none of these units have been tested.

2. A second test batch of bolometers has been fabricated to give ten identical units for each of the four gallium-doped germanium samples, as follows:

Crystal No.	Supplier	Crystal Resistivity Range (ohm cm)	Die Size (inches)	Leads (inches, Karma)
1	Knapic	0.83 to 1.05	0.040 x 0.080 x 0.003	0.002
2	Sylvania	0.42 to 0.52	0.040 x 0.080 x 0.005	0.002
3	Semi Metals	0.27 to 0.30	0.040 x 0.080 x 0.005	0.002
4	Leytess	0.165 to 0.185	0.040 x 0.080 x 0.005	0.002

The fabrication techniques have been standardized reasonably well, so that bolometers of almost any desired configuration can now be fabricated reliably. No further effort will be made to develop fabrication techniques until the two batches described above have been tested.

B. BOLOMETER MEASUREMENTS

1. Characterization of Germanium Resistance vs Temperature Curve

The single most meaningful measurement characterizing the germanium material is its resistance as a function of temperature. In general, the steeper the slope of this resistance-temperature curve, the better the performance of the bolometer.

The resistance-temperature relationship has been described in models governed by equations of the form

$$R = C_1 T^{-A} \tag{1}$$

or,

$$R = C_2 \exp(-B/T) \tag{2}$$

or a combination,

$$R = C_3 T^{-D} \exp(-E/T). \tag{3}$$

The sensitivity is given by the slope dR/dT, or, normalized for resistance, by

$$S = \frac{1}{R} \frac{dR}{dT}$$

Depending on the particular model, the sensitivity may maximize at some temperature, $T_{s_{max}}$, which is obtained by setting $\frac{dS}{dT} = 0$, provided that $\frac{d^2S}{dT^2}\Big|_{T_{s_{max}}}$ is negative.

For Equations 1—3:

(1) $R = CT^{-A}$

$$S = -\frac{1}{R}\frac{dR}{dT} = \frac{A}{T}$$

$$\frac{dS}{dT} = -\frac{A}{T^2} \neq 0$$

(2) $R = Ce^{-\frac{B}{T}}$

$$S = -\frac{1}{R}\frac{dR}{dT} = -\frac{B}{T^2}$$

$$\frac{dS}{dT} = \frac{2B}{T^3} \neq 0$$

(3) $R = CT^{-D}e^{-\frac{E}{T}}$

$$S = \frac{1}{R}\frac{dR}{dT} = DT^{-1} - ET^{-2}$$

$$\frac{dS}{dT} = -D^{-2} + 2ET^{-3} = 0 \text{ for } T_{s_{max}} = \frac{2D}{E}$$

Checking: $\left.\frac{d^2S}{dT^2}\right|_{T_{s_{max}}} = -\frac{1}{8}\frac{D^4}{E^3} < 0$, since D, E are positive numbers.

Equation Forms 1 and 2 are useful for "quick-look" evaluations of the smoothness of a set of observational data where the values of A or B are computed for adjoining pairs of data points and plotted appropriately. Also, comparison can be made readily with the data of other investigators who use these equation forms. Taken point by point, Equation 2 has some physical significance, since stepwise behavior of B should characterize particular impurities active over limited temperature ranges.

Equation 3 appears to provide a more accurate characterization of R(T) for wide temperature ranges; one group of investigators has reported an accuracy of $\frac{\Delta T}{T} \lesssim 0.24\ \%$ over the temperature range

1.2 to 4.2° K for fifteen gallium-doped germanium thermometers.[2] Hence, a least squares fit to the data points should give values of the parameters C, D, and E; this would be useful for selection of that portion most suitable for bolometer fabrication from a large batch of material, as well as for prediction about the performance of bolometers.

For all three equation forms, one should seek a material having large values of A, D and/or small values of B, E in the temperature range of interest.

Preliminary measurements have been made of the bolometer and the germanium material properties in two uses: 1) with a Texas Instruments dewar, and 2) with a laboratory glass dewar. These are discussed below separately.

2. Measurements Using the Texas Instruments Dewar

a. Apparatus and Procedure. The first measurements were made using the Texas Instruments (TI) Dewar. Five identical bolometers, fabricated from Leytess material (see I-2 above), were mounted on the inner flask base in the vacuum jacket so that their field of view was restricted entirely to blackened material at the heat-sink temperature; their thermal conductance to the heat sink was about 5×10^{-7} watts/° K.

The bath temperature was obtained by reading the bath vapor pressure in the two following ways: a double-tee fitting was fabricated for the dewar outlet so that the pumping flow was straight through the fitting. The first tee went directly into the pumping line; the second tee was connected to a capillary tube that passed through the dewar outlet into the upper region of the inner flask. It was expected that readings from the first tee would show pressure losses due to the pumping flow rate, even under constant temperature conditions, and that readings from the capillary would indicate the true bath pressure.

Voltage vs current readings were taken at very small current values with both positive and negative polarities to obtain the slope of the curve at zero current, i.e. the bolometer resistance at the bath temperature. The larger values of current would then give the normal load curve from which the bolometer responsivities could be calculated. Hence, one set of measurements would yield the following:

(1) A straight line fitted through the very low current values of both polarities would indicate that the load curve passed through zero and would verify that the lead attachments were, indeed, purely ohmic in character;

(2) the slope of the straight line would give a reasonably accurate measure of the bolometer resistance at the bath temperature;

(3) the larger current values would enable calculations of the responsivity as a function of bias current, giving the peak responsivity, as well as

(4) the bias current range for peak responsivity.

The measurement procedure began at about 4.2° K, with atmospheric pressure on the bath. Bias currents were set on one bolometer point-by-point and the resulting voltages were read. This procedure was repeated for each bolometer. The bath was then pumped down to the appropriate pressure for the next desired temperature, the pumping line was throttled to establish equilibrium, and the readings were made at that temperature.

b. Results. The first set of data was taken at temperatures of 4.20, 3.50, 3.00, 2.50, 2.00, and 1.57 °K at at minimum currents of 0.25 μamps at 4.20°K down to 0.05 μamps at 1.57°K. Calculated values of A (Eq. Form 1) ranged from 3.0 to 4.5 for all five bolometers.

The second set of data was taken at smaller current values (0.0025 μamps at each temperature) and at temperatures below the liquid helium λ-point at 2.10, 2.00, 1.90, 1.80, 1.70, 1.60, and 1.55°K. Calculated values of A fell in the range 3.5 to 5.0. Calculated values of the responsivity were on the order of 1×10^6 v/w.

For the first two sets of data the pressure was read only at the tee into the pumping line. Precautions to eliminate formation of ice plugs in the capillary tubing from the second tee into the bath volume were insufficient. The current values used for these two sets

overlapped in only a few cases, but comparison of the voltages at comparable temperatures and currents showed differences of about 10%. It was suspected that this was caused by errors in reading the bath pressure.

A third run was made at 2°K using the capillary tap for pressure reading and a large bias current range of 40 points (from 0.05 to 5.00 μamps) to obtain better data for responsivity calculations. At comparable temperatures and currents, these voltage readings agreed to within about 5 % with those of the first two sets. Calculated maximum responsivities were near 1 x 10^6 v/w, although the peak values occurred at somewhat lower than expected bias currents.

A fourth run was made, repeating the conditions of the third run. The voltage readings differed from those of the preceding runs by large factors under supposedly comparable conditions of bias current and bath temperature. Again, there were substantial difficulties in obtaining definite bath pressure readings.

c. Conclusions. The principal conclusions derived from these four runs were that the bath pressure—and hence the bath temperature—was not being repeated and that this was largely due to the inner flask access tube geometry ($\frac{1}{4}$-inch diameter and 5-inch length) of the TI dewar.

The secondary conclusion was that the bolometer characteristics appeared to be reasonably satisfactory for the first five units tested. The tentative values of resistance vs temperature curve exponents (Eq. Form 1) for individual bolometers were in the range A = 3 to A = 4.5, and tentative responsivities (near 1 x 10^6 v/w) indicated that these bolometers could be useful units.

For the following reasons, the tests were transferred from the TI dewar to a larger, nitrogen-shielded glass dewar:

(1) The much larger (2-inch diameter) pumping line would give much higher pumping speeds into the helium flask, thus yielding lower temperatures.

(2) A variety of experiment sample arrangements would be possible so that either finished bolometers or whole germanium wafers could be immersed directly into the liquid, or finished bolometers could be contained in a vacuum space with or without incident radiation. In particular, the resistance vs temperature curves should be determined with the sample fully immersed in the liquid bath to insure that the germanium is at the bath temperature.

(3) The ample size of the glass helium dewar would allow a variety of methods of measurement and cross-checking of the bath temperature.

3. Measurements Using the Glass Dewar

a. Apparatus and Procedure. In transferring the five bolometers to the sample mounts for the glass dewar, two of the bolometers' lead wires broke off. One new bolometer of the same batch (Leytess) was mounted, giving a total of four.

Bath pressure readings were made in two ways:

(1) A $\frac{3}{8}$-inch-diameter tube was attached to the experiment tower mounting plate. This tube was used to fill the inner dewar with liquid helium and as a pressure tap into the relatively "dead" region several inches above the flow path out the bath pumping side arm.

(2) A closed-volume, helium vapor pressure "thermometer" was fabricated so that a $\frac{1}{16}$-inch stainless steel tube passed down the experiment tower, terminating in a copper bulb on the dewar vertical axis and at the level of the samples. The upper end of the tubing was connected via a $\frac{1}{4}$-inch rubber vacuum hose to two pressure gauges,* a supply of gaseous helium, and a

---

* Wallace and Tiernan Absolute Pressure Gauges (Type FA-160) with ranges of 0—800 mm Hg in 5-mm graduations and 0—50 mm Hg in 0.2-mm graduations.

vacuum source. Prior to filling the dewar with liquid helium, the thermometer system volume was evacuated and filled with dry helium gas at least three times up to a positive pressure of 5 psi.

The electrical system used in testing the bolometers is shown in Figure 1. It consists of a stable reference voltage source, a ten-megohm resistor, and voltmeters to measure the reference voltage and the voltage across the bolometer. A switching arrangement allows the observer to connect the system to each bolometer in sequence. A Vidar model 260 voltage-to-frequency converter with an input impedence of 1,000 megohms was used to avoid loading errors when measuring the voltage across the bolometer. The output signal had a scale factor of 100 KHz/volt that was converted to a voltage indication, readable to one part in 10^5 using a digital counter. The bolometer resistance can then be calculated from V_{Ref}, V_{Bolo}, and R_L.

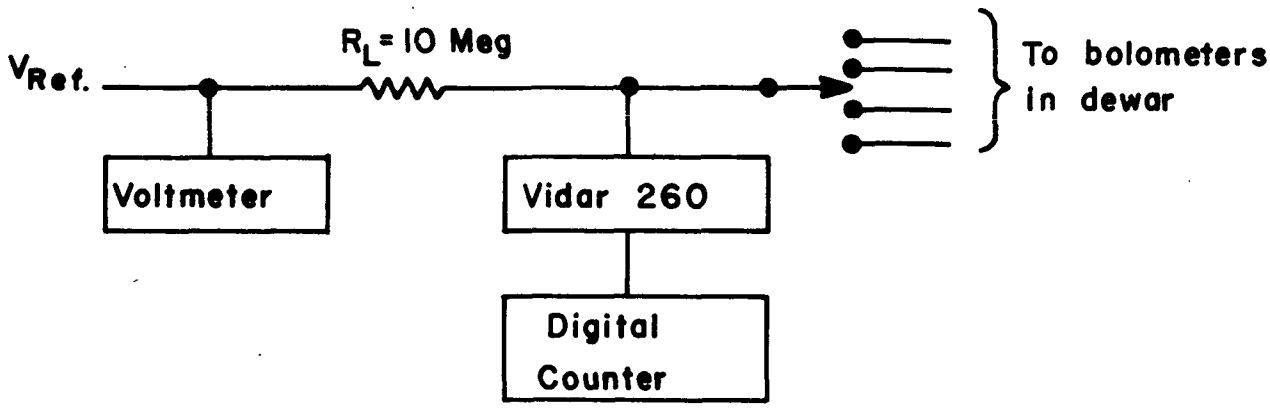

FIGURE 1

Bolometer Test Set-Up

For the two runs made to date the temperature was varied from 4.2°K down to 1.45°K, and the resistance for each unit at each temperature point was measured when equilibrium had been established. Equilibrium was determined by decreasing the bath pressure and then leveling it off at the desired pressure until the bolometer voltage changes averaged about 1 part in 10^3 per second.

The random fluctuations in the voltage, particularly at lower temperatures, were great enough to make it somewhat difficult to determine when the readings no longer exhibited a trend. In subsequent measurements either a digital printout or an analog trace of the bolometer voltage will be used to determine when the bath temperature attains equilibrium.

The voltage readings at each temperature point were used to calculate resistance. The resistance values were then used to calculate A for the equation form $R = C_1 T^{-A}$ and B for the form $R = C_2 \exp(-B/T)$ for each succeeding pair of points.

Figure 1 is a semi-log plot of R vs 1/T from both runs for Bolometers 1, 2, and 3. Bolometer 4 data were omitted from the plot for clarity because the data points were almost coincident with those of Bolometer 2. This method of plotting the data was selected because constant values of B that characterize a particular impurity appear as a straight line over the appropriate temperature range for that impurity.

The derived parameters A and B were plotted (Figure 2) to determine how well the simple equation forms fit the observed data. Note that the points were derived by taking pairs of resistance values in turn and were plotted at temperatures midway between the observed data points. The patterns of plotted data were quite similar for all four bolometers, therefore only the plot for Bolometer 1 is presented.

b. Results and Conclusions. The figures illustrate several features of interest:

(1) The data from 1.8°K to 1.45°K in Figure 1 differ by 3% or less between the two runs. The larger differences of about 12% for the points at 1.9, 2.0, and 2.1°K were expected due to

problems with the closed-volume thermometer during the first run. Apparently the volume was overfilled with gas before the run, so that the liquid level rose above the bulb into the capillary tubing, and erroneous pressure readings resulted. At 1.8 °K the pumping line was closed to stop the flow and the thermometer was vented momentarily into the bath volume. Subsequent readings were identical for the thermometer and the bath volume-pressure tap under low flow-rate conditions. A similar technique gave identical readings for both pressures for all points of the second run.

(2) The values of resistance and the temperature exponent A are comparable to those of usable bolometers produced by others. For example, Low [3] reported a value of A = 3.85 and R = 2×10^4 ohms at a temperature of 2.15 °K. All four of the bolometers tested had values of A from 4.4—4.6 at T = 2.10 °K.

(3) Figure 2 indicates the relative smoothness of Run 2 data as compared to that of Run 1. These plots of the parameters A and B can be readily made and serve as useful indicators of the reliability of a set of data.

(4) The parameters A and B both indicate abrupt slope changes near the helium λ-point that are not understood at the present time. The data of other investigators who are concerned mainly with thermometers appear to be somewhat smoother in this region. More investigation into the material behavior near the λ-point is required.

(5) The parameters A and B, used in the two parameter Equation Forms 1 and 2 (see page 2), do not provide accurate characterizations of the material property R = R(T) over the temperature region below 4.2 °K. Initial trials to fit the data to the three parameter equations $R = CT^{-A}e^{-B/T}$ have not been satisfactory; more work with additional data is required to provide the most useful expression.

II. LOW NOISE AMPLIFIERS

A. DISCUSSION OF AMPLIFIER REQUIREMENTS

Any amplifier used in conjunction with a detector must have noise characteristics that complement the detector, so that the noise contribution of the amplifier is small compared to that of the detector. Table 1 lists the parameters for several bolometers.

The noise equivalent power (NEP) of a bolometer may be defined as the rms value of the sinusoidally modulated radiant power falling upon a detector that gives rise to an RMS signal voltage equal to the rms noise voltage from the detector. Low and Hoffman [4] have shown that the NEP may be computed from the expression:

$$NEP^2 = \frac{4kTR}{S^2} + 4kT^2G + 8\epsilon\sigma kAT^5 + 8\epsilon\sigma kAT_b^5 \sin^2 \frac{\varphi}{2} \qquad (1a)$$

$$= 12kT^2G + 8\epsilon\sigma kA\left(T^5 + T_b^5 \sin^2 \frac{\varphi}{2}\right) \qquad (1b)$$

where a post detection bandwidth of unity is assumed. In Equation 1a. the first term is the square of the Johnson noise voltage across the bolometer of resistance R at temperature T, divided by the square of the responsivity S. The Boltzmann constant is denoted by k. The second term is the square of the temperature noise power, where G is the thermal conductance between the heat sink and the sensing element. The third term arises from random fluctuations in the emission of the sensing element, This element, of area A, is assumed to radiate at all wavelengths with an average emissivity ϵ, and σ is the Stefan-Boltzmann constant. The fourth term represents the noise in the incident radiation originating from a blackbody background at temperature T_b. The detector is taken to be Lambertian, and the angle φ defines the size of the cone that accepts the background radiation.

Equation 1b is obtained by substituting (2) into 1a

$$S_{max} = 0.7 \left[\frac{R}{TG}\right]^{\frac{1}{2}} \qquad (2)$$

where (2) is the expression for the maximum value of the responsivity as determined by Low [3].

Since the bolometer noise voltage is the product of its NEP and responsivity, we may examine the relationship of these parameters in Figure 3, which also includes points for the bolometers of Table 1. One desires to obtain bolometers having the lowest NEP, since this implies an ability to detect the faintest objects. As long as improvements in NEP are matched by improvements in responsivity, the noise voltage from the bolometer remains constant and the same amplifier continues to be equally useful. It is expected that a practical limit will be reached for responsivity, however, so that NEP improvements for the system can only be made by improvements in the amplifiers.

If we wish the amplifier to increase the system noise voltage by only 10% over the noise voltage seen for the bolometer alone, then

$$V_{system} = \left[V_{bolo.}^2 + V_{amp.}^2\right]^{\frac{1}{2}} \text{ for uncorrelated noise, and}$$

$$V_s^2 = V_b^2 + V_a^2 = (1.1\, V_b)^2 = 1.21\, V_b^2$$

$$V_a = \sqrt{.21}\; V_b = 0.44\, V_b$$

so that the amplifier noise voltage need be only about half the bolometer noise voltage. Similarly, for a 1% amplifier contribution, the amplifier noise voltage must be only 15% of the bolometer noise voltage.

Examining some typical values, we are currently using an Ithaco Model 6051-80 low-noise preamplifier with a noise voltage of 16 nanovolts and a noise current of 10^{-14} amps. With a one-megohm input impedance (equal to the bolometer nominal resistance), we have a total amplifier contribution of 19 nanovolts. Hence, connected to a bolometer of 43 nanovolts, noise voltage, the system output would be increased 10% to 47 nv. This implies that we could investigate the noise mechanisms in a bolometer of 43-nv noise voltage to 10% accuracy, and for a responsivity near 1×10^6 v/w, our best NEP would be about 5×10^{-14} watts.

Considering the case for the preamplifier of Biard[8] as representative of current amplifier state-of-the-art, we take an amplifier noise voltage of 4.0 nv $\sqrt{\text{cps}}$, and assume a noise current of 1 femto amp/ $\sqrt{\text{cps}}$. For a 10% system, our bolometer characteristics would be: $R = 1 \times 10^6$ ohms, $v_{noise} = 9.4$ nv, and for $S = 1 \times 10^6$ v/w our best NEP would be 1×10^{-14} watts.

Now in order to attain a 10% system operating at NEP = 1×10^{-15} watts with a bolometer of $S = 1 \times 10^6$ v/w and $R = 1 \times 10^6$ ohm, we require an amplifier of 0.4 nv / $\sqrt{\text{cps}}$ noise voltage and 0.1 femto amp/ $\sqrt{\text{cps}}$ noise current. Such an amplifier does not exist.

An investigation into the noise characteristics of various types of semiconductors and amplifiers has shown that only two basic amplifier classes are capable of equivalent input noise voltages of 10 nanovolts/ $\sqrt{\text{cps}}$ or less at the low frequencies (0—100 cps) of concern. They are 1) cooled FET amplifiers, and 2) parametric amplifiers.

B. AMPLIFIER CHARACTERISTICS

1. Field effect transistors have characteristics that are particularly suitable for low-noise amplifiers at low and medium frequencies, and thus are suited for our bolometer preamplifiers. A brief review of FET characteristics follow:

The field effect transistor is based on voltage control of majority carrier flow through a semiconductor channel. The effective width—and also the conductance of the channel—is varied by the reverse potential of the gate-channel junction.

There are two distinctly different modes of operation of the FET: (1) for zero or small voltages across the channel, where the conductance of the channel is not markedly changed by the current flow, and (2) in saturation (or pinch-off), where the channel conductance is affected by the current flow so that the current becomes virtually independent of the drain voltage. In the first mode the device can be considered as a passive element controlled by the gate voltage. In the second, it appears as a three-terminal active device with characteristics similar to those of a vacuum pentode or a bipolar transistor. It is the second region of operation that is of interest to us. In the common source configuration the device has a high-input inpedance

(at least 10^7 ohms shunted by 1 to 30 pf). The output circuit is equivalent to a resistance ranging from 5 to 400 kohms shunted by a current generator of magnitude

$$I_g = g_m v_g \tag{3}$$

where g_m is the transconductance of the device and v_g is the signal voltage at the gate (see Fig. 4).

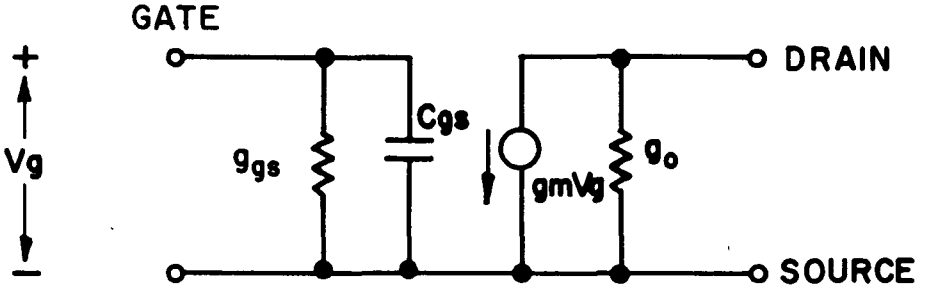

For most devices, a good approximation for the transconductance is

$$g_m \approx g_{mo} \left(\frac{I_d}{I_{do}}\right)^{\frac{1}{2}} ,$$

or

$$g_m \approx g_{mo} \left(1 - \frac{V_g}{V_p}\right) \tag{4}$$

where I_d and V_g are the magnitudes of the quiescent drain current and gate to source voltage, respectively, in the saturated region of the static characteristics. V_p is the pinch-off voltage. I_{do} and g_{mo} are the values of I_d and g_m with $V_g = 0$.

There have been many theories proposed to describe the noise characteristics of FETs. Unfortunately no theory adequately describes the magnitude of the low-frequency noise, which is, unfortunately, very pronounced in our desired operating range of frequencies. There is, however, an empirical method for finding the noise model of the FET that uses the manufacturer's published data.

Any 2-port network can be characterized by a noise model consisting of an equivalent noiseless network with noise and current generator placed at the input. These generators are independent of the circuit outside the network (see Fig 5).

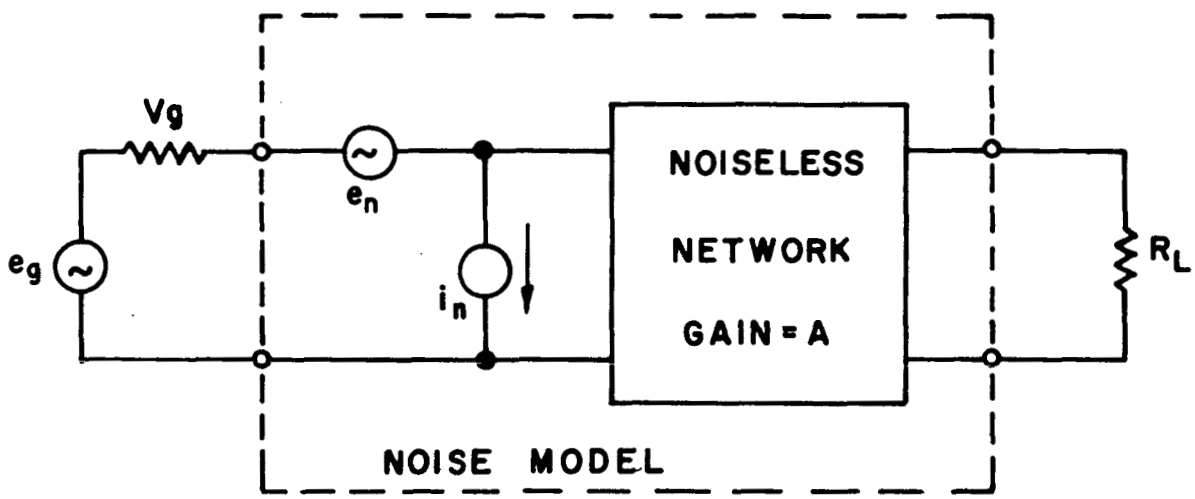

Fig. 5 Equivalent circuit of a 2-port network

e_n and i_n shall be used to represent the rms values of the noise voltage and current respectively.

The low-frequency spectrum, where one or both of the noise generators may show a 1/f dependence, is of interest. It is possible to measure e_n and i_n separately. From these values the noise figure for any generator magnitude may be calculated:

$$NF = 10 \log \left[1 + \frac{1}{4kTR_g} (i_n R_g + e_n)^2\right] \quad (5)$$

For currently available silicon devices operating at low temperatures the transconductance increases slowly to 2—3 times its room temperature value and then drops off rapidly. The peak in transconductance occurs at approximately —150 °C. Noise contributions due to gate leakage and channel conductance decrease linearly with temperature. 1/f noise decreases only slightly with temperature however, since the 1/f noise mechanism is not gain dependent and, with the increasing available gain with decreasing temperature, the effective input noise voltage decreases as does the noise figure. The most suitable amplifier configuration for our purposes is shown in Fig. 6.

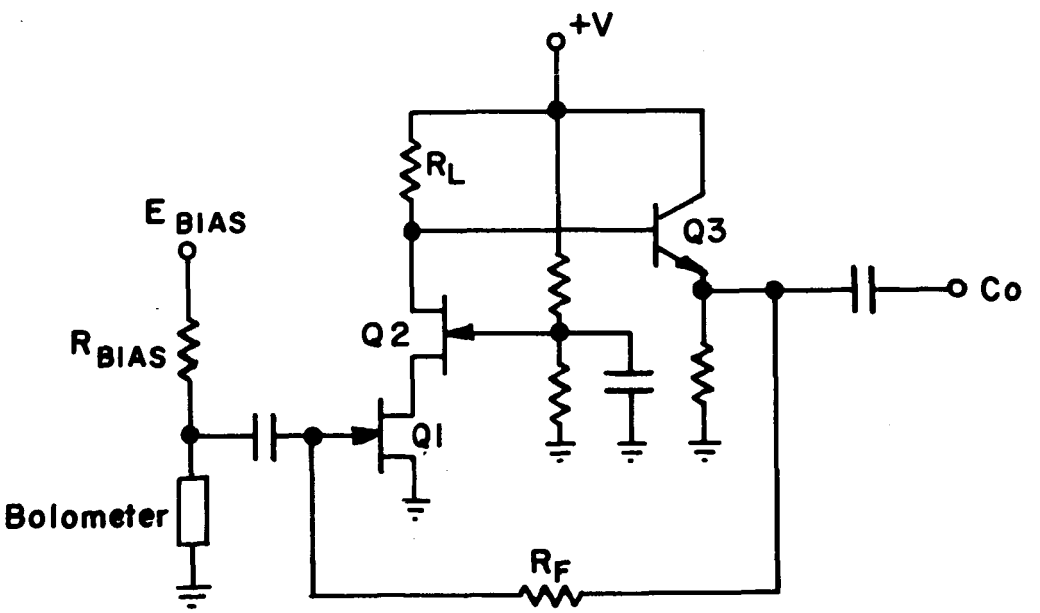

Fig. 6 Simplified schematic of preamplifier

The cascode preamplifier has both a high available gain and a low noise figure. An emitter follower isolates the cascode stage from external load changes.

The approximate gain of the amplifier is $G = g_{m(Q1)}R_L$. Thus by increasing R_L we can make the gain as high as desired.

Because of the cascode configuration, the noise contribution due to Q_2 is negligible. The noise contribution due to Q_1 can be represented by a noise current and noise voltage, as discussed above. Thus the noise characteristics of the overall amplifier can be c calculated.

2. Parametric Amplifiers

Parametric amplifiers may be used to alleviate the problem of 1/f noise—so prominent in transistor or vacuum-tube low-noise amplifiers. The circuit to be discussed is a four-frequency reactance amplifier that takes the form of a double sideband up-converter or modulator. A band of signal frequencies from dc to about two-hundred cycles per second is used to modulate an RF carrier. This amplifier differs from a resistive diode modulator in that the diodes are always reverse-biased. The nonlinear element in this case is the junction capacitance of the reverse-biased diodes. Both voltage amplification and transducer power gain are obtained. Biard [8] has reported equivalent input noise voltages of 4 $nv/\sqrt{cps}$.

Fig. 7 shows the significant frequencies used in the parametric amplifier. Operating power is supplied in the form of an RF carrier from the pump that modulates the transition capacitance of the varactor diodes. The pump angular frequency is denoted by $\overline{p}$. Input signal is provided at an angular frequency $\overline{a}$ while the amplifier output is developed at the sum and difference sidebands $\overline{s} = \overline{p} + \overline{a}$ and $\overline{d} = \overline{p} - \overline{a}$.

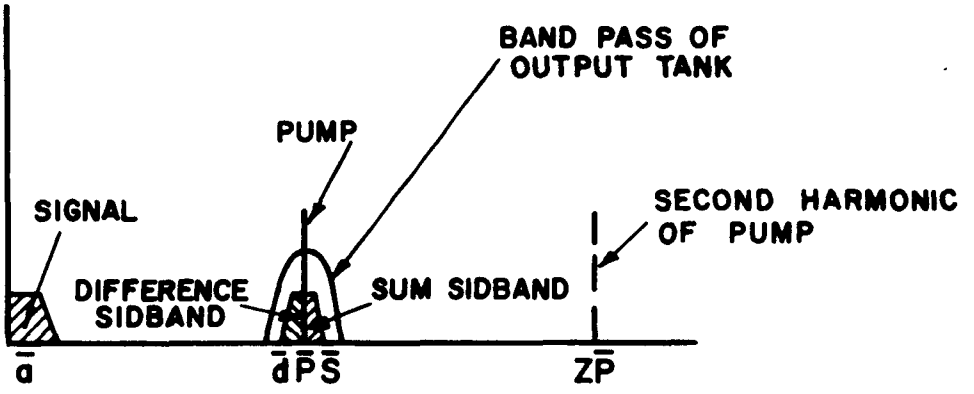

Fig. 7 Significant frequencies of the parametric amplifier

The Manley-Rowe power relations, which describe the power relationships between the pump, frequency, the signal frequencies, and the output frequencies become

$$\frac{W_a}{\bar{a}} + \frac{W_s}{\bar{s}} - \frac{W_d}{\bar{d}} = 0 \tag{6}$$

and

$$\frac{W_p}{\bar{p}} + \frac{W_s}{\bar{s}} + \frac{W_d}{\bar{d}} = 0 \tag{7}$$

where W_x represents power supplied to the varactor at angular frequency $\bar{\omega} = \bar{x}$ (x = a, s, or d).

From (6) power delivered to a load at $\bar{s}$ reflects a positive resistance or loading effect at signal frequency, while power delivered to a load at $\bar{d}$ presents a negative resistance or regenerative action at signal frequency. From (7) both sidebands appear as a positive resistance and, thus, a load at pump frequency.

The useful output signal is represented as the sum of the upper- and lower-sideband power. The power gain of the amplifier is

$$G = -\frac{W_s + W_d}{W_a} = \frac{\bar{s}}{\bar{a}} \frac{1 + \frac{W_d}{W_s}}{1 - \frac{\bar{s} W_d}{\bar{d} W_s}} \tag{8}$$

For

$$\bar{s} W_d = \bar{d} W_s \tag{9}$$

the power gain increases without limit, and (6) reduces to $w_a = 0$, which implies zero conductance at signal frequency. This condition is met in our amplifier, since the pump frequency is very much higher than the signal frequency.

Figure 8 is a block diagram of the parametric amplifier.

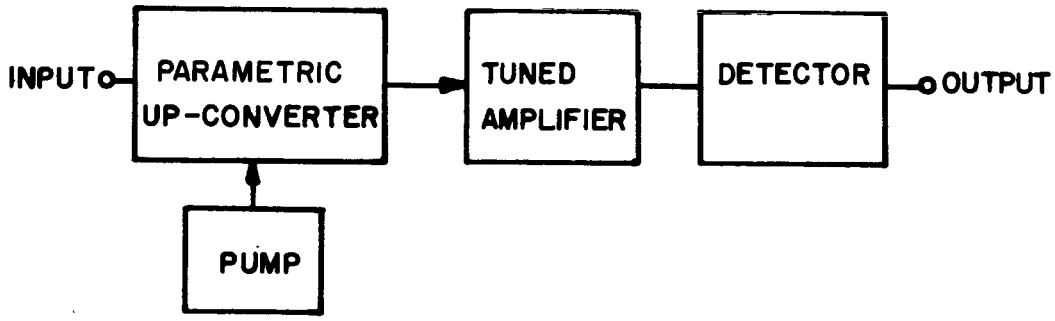

Fig. 8 Block diagram of parametric amplifier

The parametric amplifier operation is as follows: The pump signal is modulated by the input signal in the parametric up-converter, the amplitude-modulated output signal of the reactance amplifier is further amplified by the tuned amplifier, and, finally, the signal is demodulated to recover the input signal.

There are several major noise sources in the parametric amplifier: 1) pump noise, 2) thermal noise in the parametric up-converter tuned circuit, and 3) noise in the first stage of the tuned amplifier.

Pump noise can be reduced by a factor of at least 50 using a crystal oscillator instead of RC or LC oscillators for the pump oscillator. The effect of the pump noise can be reduced by optimizing the balance of the parametric up-converter.

The thermal noise in the parametric up-converter tuned circuit can be reduced by cooling the circuit to cryogenic temperatures. The resistance of ordinary varactor diodes increases by a factor of four when cooled to 77° K, so that noise contribution remains constant and only the inductor noise temperature is substantially reduced; however, by using GaAs varactor diodes or silicon varactors doped for low-temperature operation, the noise contribution due to the varactors can also be reduced.

The equivalent input noise voltage of the first stage of the tuned amplifier can be made small enough to not affect adversly the overall noise figure of the amplifier by using a low-noise FET for the input and by proper matching to the source resistance.

C. CONCLUSIONS

Because of the relative simplicity of a cooled FET preamplifier, a thorough analytical study of the properties of FETs will be made. This study will include several different amplifier configurations. A search must also be made for new and better types of FETs for the input stage of the amplifier.

However, all semiconductor devices have a 1/f component of noise, and the noise-voltage output of our best bolometers should approach 1 nv. Hence, we may find that we cannot build a cooled FET with the required

equivalent input noise voltage to complement our bolometers and will then have to consider an advanced parametric amplifier. The parametric amplifier does not have a large 1/f noise component and theoretically, can have a very low equivalent input noise voltage. It is a very complex device, however, and will be considered in detail only when the cooled FET approach is no longer profitable.

III. PROGRAM CONTINUATION

The objectives for the next period include:

1. measurement of R(T) for the germanium on hand (measurements of the completed bolometers of the second test batch will be continued, and then whole wafers will be studied),
2. procurement and measurements of additional germanium samples as indicated by the results from objective #1,
3. fabrication of an evacuated experiment space in the glass dewar to enable
4. measurement of responsivity, time constant, and NEP for the bolometers selected as most promising from the R(T) results, and
5. continued study of the bolometer-preamplifier relationship, aimed at providing a system of high sensitivity, with the intrinsic bolometer noise being the dominant noise factor. While this will involve some empirical study of bread-boarded circuits or selected components, the main emphasis will be toward understanding the processes involved.

The primary demand for experimental time will be on measurements of the germanium properties. For example, reference to Figure 3 indicates that should bolometer material become available that yields responsivities substantially greater than the present practical range near 1×10^6 v/w, systems having NEP $\cong 10^{-15}$ watts would be feasible with preamplifiers near the current state-of-the-art. However, should responsivities near 1×10^6 v/w prove to be a practical upper limit, then preamplifiers with noise voltages less than nv would be essential for realization of the foreseen bolometer potential of 1×10^{-15} watts NEP.

REFERENCES

1 Space Sciences Laboratory Semi-Annual Progress Report. Series No. 7, Issue No. 50, September 30, 1966, pg. 230.

2 Clairborne, L. T., W. R. Hardin, and N. G. Einspruch. Low temperature Germanium Resistance Thermometry. Rev. Sci. Instr. 37 (10): 1422 (October 1966).

3 Low, F. Low Temperature Germanium Bolometer. J. Opt. Soc. Am. 51: 1300 (1961).

4 Low, F., and A. R. Hoffman. The Detectivity of Cryogenic Bolometers. Applied Optics 2: 649 (1963).

5 Englesrath, A., and E. V. Lowenstein. Comparison of Characteristics of Far Infrared Detectors. Paper FD-15, Annual Meeting of the Optical Society of America (October 1965).

6 Low, F. Performance of Thermal Detection Radiometer at 1.2 mm. Proc. IEEE 53: 516 (1965).

7 Eisenman, W. L. Properties of Photodetectors. NOL-C Report 691 (November 15, 1966).

8 Baird, J. R. Low Frequency Reactance Amplifier. Proc. IEEE 51, 298 (1963).

PERSONNEL

Professor Harold Weaver	—	Principal Investigator
Wilkie Talbert	—	Associate Development Engineer
Michael Parmett	—	Assistant Development Engineer

TABLE 1: TABULATION OF BOLOMETERS

	Stratoscope*			Low[3] (1961)	Englesrath and Lowenstein[5] (1965)	Low[6] (1965)	Eisenman[7] (1966)
	Bolometer A	Bolometer B	Bolometer C				
Temperature (°K)	2.0	2.0	2.0	2.15	1.3	2.0	4.2
Time Constant (sec)	5×10^{-3}	5×10^{-3}	5×10^{-3}	4×10^{-4}	6×10^{-4}	12×10^{-3}	7×10^{-3}
Length (mm)	1.0	1.0	1.0	na	na	1.2	2.0
Width (mm)	0.60	0.30	0.15	na	na	1.0	2.0
Thickness (mm)	0.03	0.03	0.03	0.12	0.15	0.36	
Area (cm^2)	0.006	0.003	0.0015	0.15	0.1	0.012	4×10^{-2}
Thermal Conductance, G (W/°K)	1×10^{-6}	5×10^{-7}	2×10^{-7}	1.83×10^{-4}	0.60×10^{-4}	0.85×10^{-6}	
NEP (watts)	3×10^{-14}	2×10^{-14}	1×10^{-14}	5×10^{-13}	1.3×10^{-12}	4×10^{-14}	4×10^{-12}
Max. Responsivity (volts/watt)	5×10^{5}	7×10^{5}	1×10^{6}	4.5×10^{3}	7×10^{4}	1.3×10^{6}	1.6×10^{5}
Noise Voltage (volt (volts) Δf = 1 cps	1.5×10^{-8}	1.4×10^{-8}	1×10^{-8}	2×10^{-9}	9.1×10^{8}	5×10^{-8}	4×10^{-8}
Nominal Resistance, (ohms)	1×10^{6}	1×10^{6}	1×10^{5}	1.2×10^{4}	0.7×10^{6}	7×10^{6}	

* These values are the design parameters for the Stratoscope II bolometers. Laboratory tests of the completed bolometers with the flight nuvistor preamplifier were limited by current noise in the input circuit to the first nuvistor. Responsivities measured were indeed near 1×10^{6} v/w, but the measured NEP's approached 3×10^{-13} watts, about an order of magnitude too large.

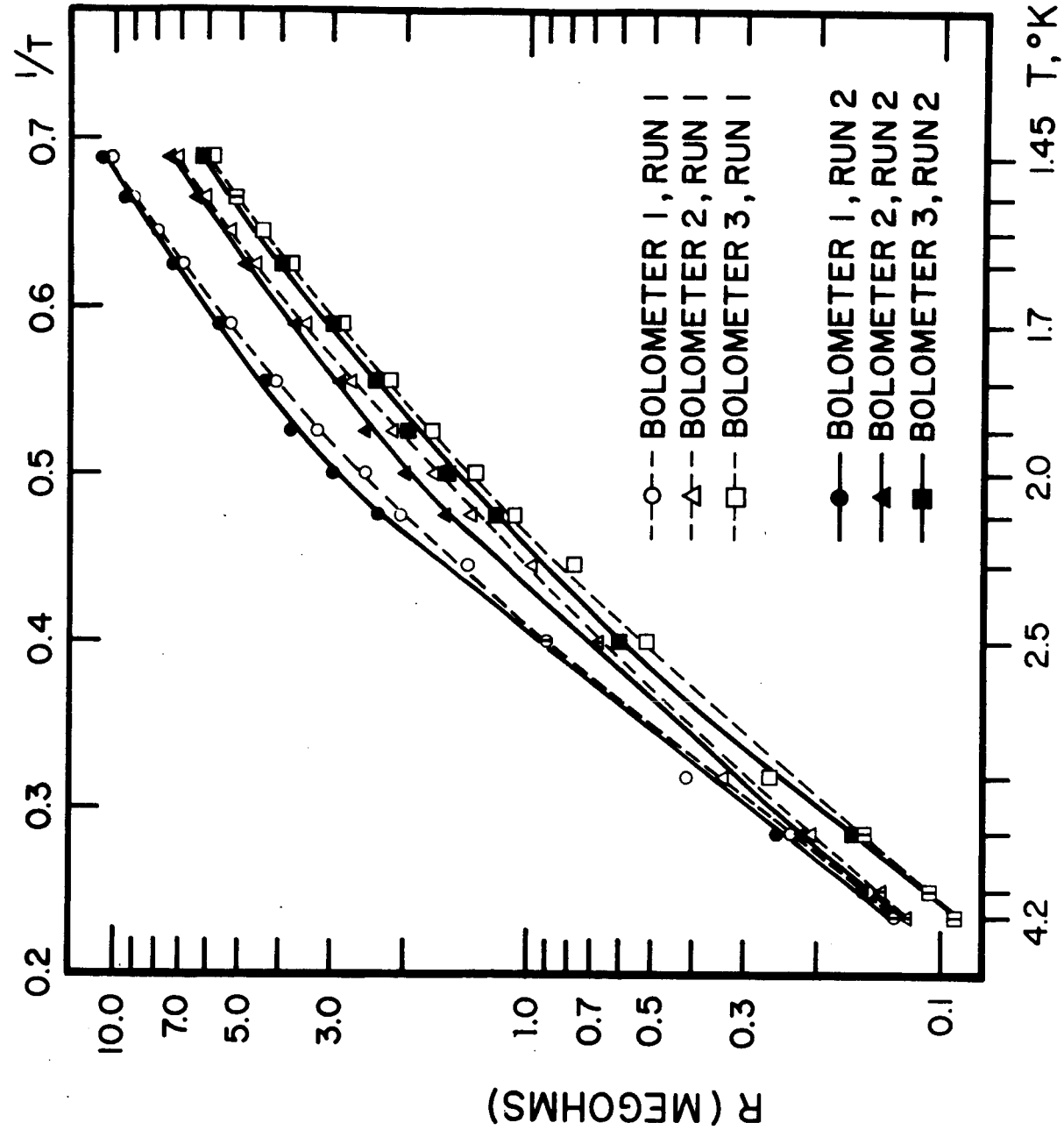

FIGURE 1. Bolometer resistance as a function of temperature.

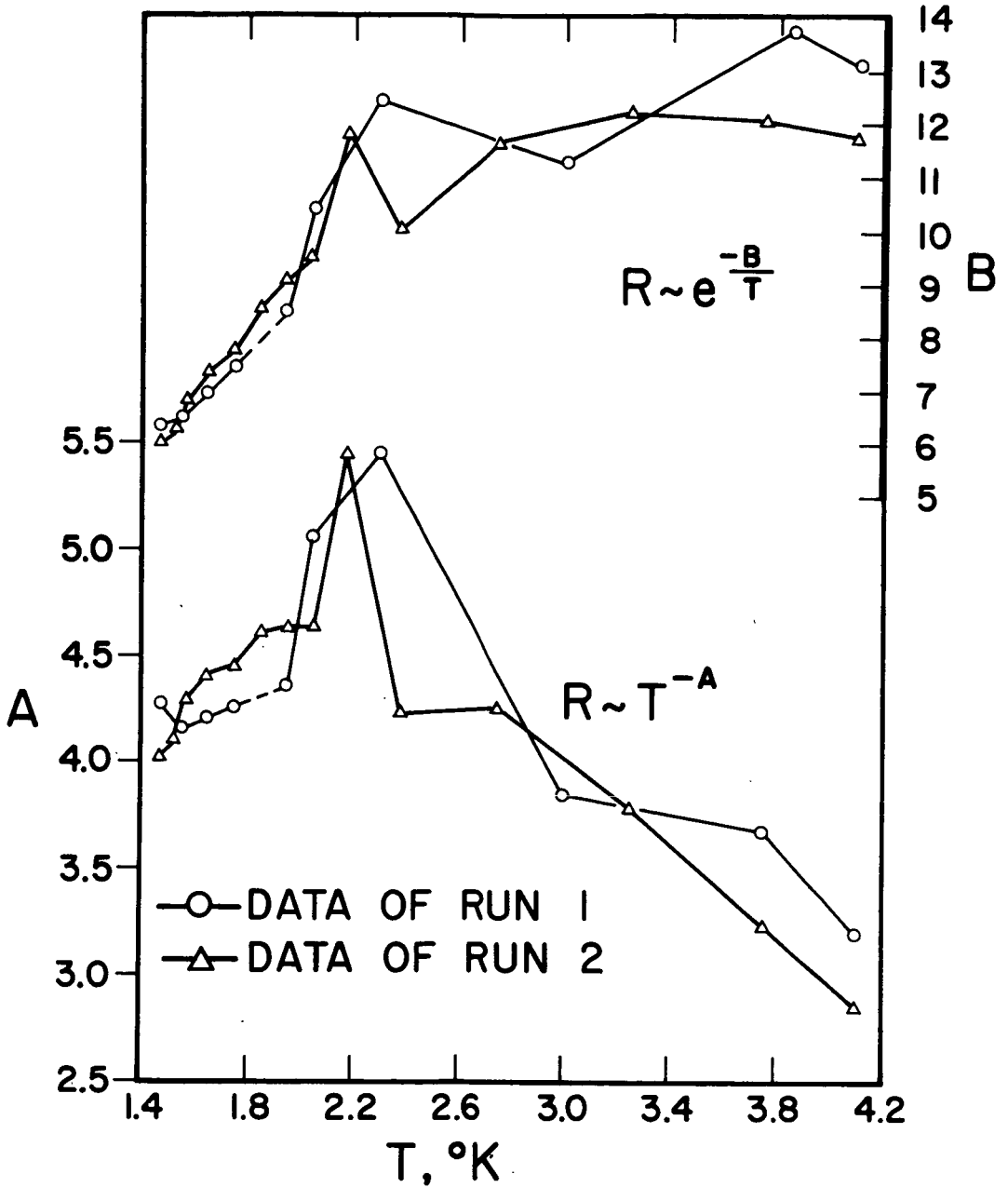

FIGURE 2. Data of Bolometer #1 Plot of Bolometer Temperature Exponents A and B for the Equations Indicated.

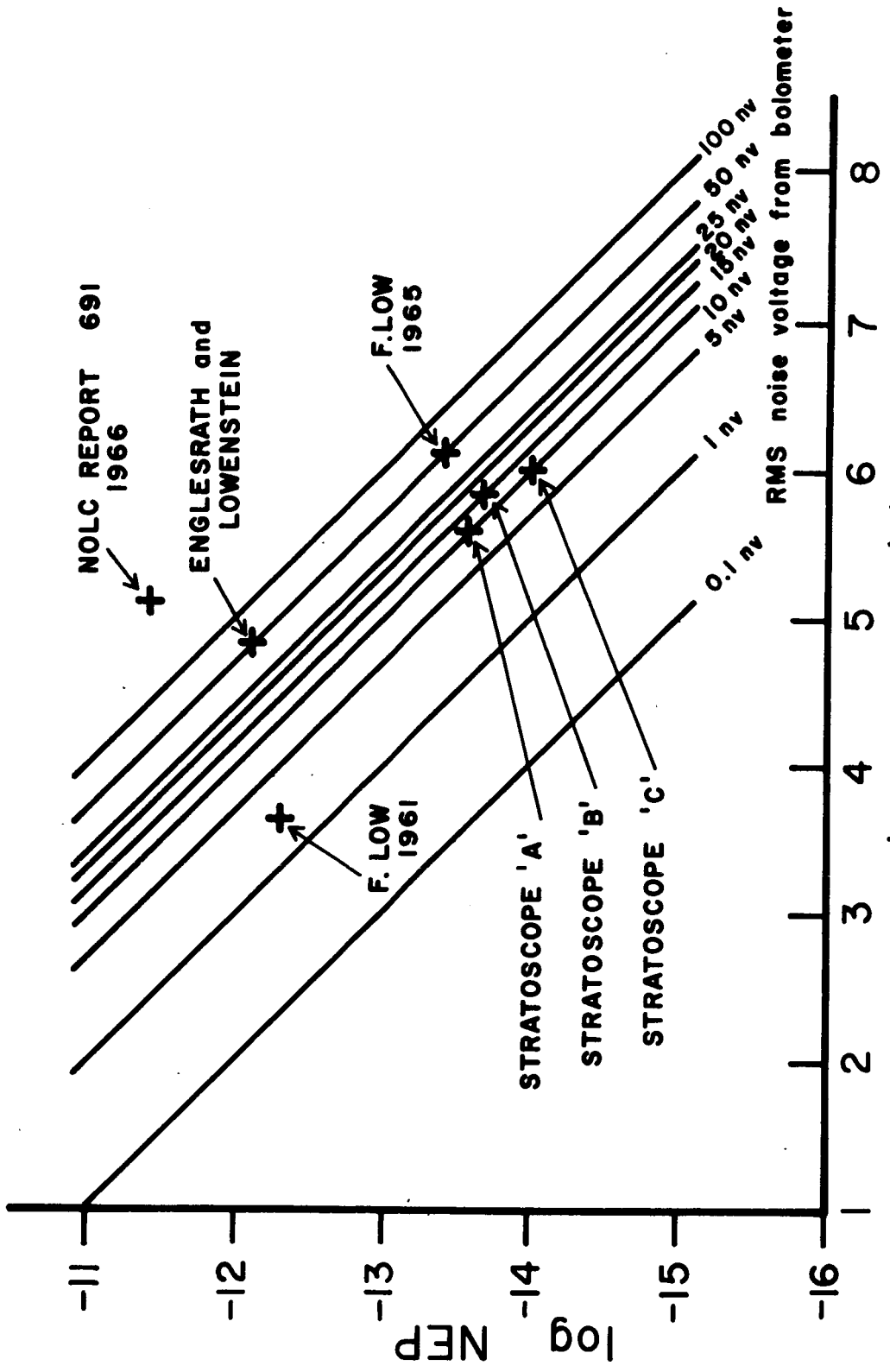

FIGURE 3. Bolometer Output Noise Voltage as a Function of Responsivity and NEP.